Ecology, 85(7), 2004, pp. 1979–1991

LOCAL FORAGING AND LIMITED MOBILITY: DYNAMICS OF A SIZE-STRUCTURED CONSUMER POPULATION

TOBIAS VAN KOOTEN,[1,3] ANDRÉ M. DE ROOS,[1] AND LENNART PERSSON[2]

[1]*Institute for Biodiversity and Ecosystem Dynamics, University of Amsterdam, P.O. Box 94084, 1090 GB Amsterdam, The Netherlands*
[2]*Department of Ecology and Environmental Science, Umeå University, S-901 87 Umeå, Sweden*

Abstract. Size-structured population models often exhibit single generation cycles, which are driven by scramble competition within a generation and size-based competitive asymmetry among generations. These cycles are characterized by the dominance of a single cohort and thus by a high degree of synchronization of the individual life histories. The models, however, do not generally allow for divergence in size among individuals born at the same time. Size divergence may, for example, result from the stochasticity that arises due to local interactions between individuals and their environment and has been shown to affect the population dynamics within generations. We studied the effect of the size divergence that develops as a result of stochasticity over many generations, considering the full population dynamical feedback, including resource dynamics. The stochastic variation in our model was generated by local interactions of individuals with the environment. We varied the mobility of individuals, which regulated the strength of the local resource feedback on the consumers. We found that at very high mobility our model provided a good correspondence to similar but fully deterministic models, showing the single generation cycles typical for a size-structured consumer–resource interaction. Intermediate levels of mobility had no notable effect on the dynamics of our model population. At very low mobility, the dynamics appeared to be strongly influenced by stochasticity. We showed that by superposition of the underlying deterministic dynamics and the stochasticity induced by local interactions we could fully understand the dynamics of the model. This finding led us to conclude that, while individual variability may have an impact on population structure and dynamics, it does not necessarily change the deterministic interactions that determine global population dynamics. More specifically, our study highlights the robustness of single generation cycles, showing that even at high levels of individual variability the population dynamics will intermittently exhibit patterns resembling these cycles.

Key words: cohort competition; consumer–resource interaction; demographic stochasticity; life-history variability; mobility; physiologically structured population models.

INTRODUCTION

Ecologists have for a long time pointed out the importance of size or physiological structure in populations (Lindström 1955, Ebenman and Persson 1988). Classical ecological theory is based on modeling approaches that describe populations in terms of density or numbers of individuals. Only recently, with the availability of new analysis and simulation tools theorists have begun to rigorously explore the dynamical consequences of physiological structure (Metz et al. 1988, de Roos et al. 1992, Gurney et al. 1996, McCauley et al. 1996, Murdoch et al. 1998). This has led to a general understanding of how size-based interactions can shape population and community dynamics (de Roos et al. 1992, 2002, Persson et al. 1998, Claessen et al. 2000, de Roos and Persson 2001). Most of the models employed in these papers are based on the formalisms and algorithms derived in Metz and Diekmann (1986) and de Roos (1989), in which a population is described by a frequency distribution over one or more physiological traits. The framework is based on an assumption that individuals born at the same time remain identical throughout life history, i.e., variability among such individuals cannot develop (Metz and de Roos 1992). While the models are formulated in terms of individual level processes, they do not consider individuals as discrete, independent units.

Another method that has gained momentum since the 1980s is the individual based simulation model (IBSM). Rather than using mathematics to arrive at an acceptable simplification of natural systems, this approach relies on computer power to simulate a large number of individuals as discrete units (for references see reviews by Tyler and Rose [1994] and Grimm [1999]). These individuals are represented by an arbitrary number of relevant individual-level variables, such as age, mass, social status, or any property important for the problem under consideration. The individual-level variables are supplemented by a set of

Manuscript received 7 May 2003; revised 1 October 2003; accepted 9 October 2003; final version received 17 November 2003. Corresponding Editor: W. S. C. Gurney.

[3] E-mail: kooten@science.uva.nl

rules defining the interaction of individuals with the environment and each other.

In contrast to structured population models sensu Metz and Diekmann (1986), these simulation models keep track of all individual-level variables for each individual separately, and are hence perfectly capable of dealing with development of variation between initially similar individuals. In our paper we use the terms variation or variability to refer to such differences between initially similar individuals. Using IBSMs, several influential papers have tackled the problem of how individual variation affects life history and population dynamics (Thompson et al. 1974, DeAngelis et al. 1979, 1993, Pacala and Silander 1985). However, as stated by Tyler and Rose (1994), these papers study the within-generation effects of individual variation on the population size distribution. More recent IBSMs do take recruitment into account (Schmitz and Booth 1997, Dong and DeAngelis 1998, Schmitz 2000), but do not explicitly study the effects of individual-level variation on population dynamics. Hence, a discrepancy exists in that generally, individual variation is considered to be an important factor in population dynamics, but all knowledge about its influence is based on within-generation modeling excercises. The long-term effects of individual variation on population dynamics thus remain largely unknown.

In this paper we study this relationship between individual variability and the global and local feedback via the population dynamics, on the individuals, bridging the gap between on one hand the modeling approaches that ignore variation between individuals and on the other hand the individual based simulation approaches. To this end, we derive a model that is based on the approach pioneered in Metz and Diekmann (1986), with the numerical integration techniques developed in de Roos et al. (1992). We adapt the model formulation to account for a one-dimensional spatially structured environment. In our model, all individuals that are born at a particular time are subdivided into a fixed number of groups (schools), which move independently through this space. While this is not an individual based simulation model sensu Huston et al. (1988), the subdivision of cohorts into schools allows for variation between individuals of the same age to develop. We consider the consumer-resource model studied in Persson et al. (1998) and de Roos et al. (2002) as a limiting case and starting point of our study. As schools of individuals move through space, they depress the resource locally. Since a location can be populated by any number of schools, containing any number of individuals, spatial heterogeneity in the resource level develops. The life history of individuals in a school depends on the resource levels it has experienced since its birth, thus the spatial heterogeneity in the resource will cause the state of individuals (e.g., their reversible and irreversible mass) to vary. We vary the extent of this divergence by varying the mobility of the schools. We analyze how the single cohort cycles that characterize the dynamics of size-structured models (Persson et al. 1998) are affected by the variation within year classes that arises when mobility of individuals is limited. Furthermore we look at the different growth trajectories exhibited by the individuals in the population, and relate these to the global population dynamics.

MODEL FORMULATION

We model the interaction between a size structured consumer and a resource following the approach developed in Persson et al. (1998) in a spatially structured environment. We use the parameter set for Eurasian perch (*Perca fluviatilis*) that is used in Claessen et al. (2000) and de Roos et al. (2002). For reference, all parameters of the model are listed in Table 1. Perch is a well-studied organism, and a very common species in temperate aquatic systems throughout Europe. The parameter set we use is valid for perch that occur in lakes in central Sweden. The growth season for perch at this latitude is 90 days, due to low water temperature and ice cover during the rest of the year. All individual level processes in the model are continuous, except reproduction and movement of consumers through space. Reproduction is a pulsed event, occurring only at the start of each growth season. For computational reasons we allow movement of consumers through space to occur once per day, at the end of the day. We use a structured environment that consists of 40 separate resource populations interlinked in a circular fashion, creating a discrete one-dimensional circular space. All resource compartments have identical characteristics and hence approach the same equilibrium resource density in the absence of consumers. Next we discuss the formulation of the three states (the *i*-state, the environment, and the population bookkeeping) used in the model.

The i-state processes

An individual, in this model, is characterized by its mass. We make a distinction between reversible mass and irreversible mass (y and x, respectively in Table 1). All other characteristics except those related to spatial position of the individual can be derived from these two quantities. Reversible mass consists of all tissue that is lost during starvation. This includes fat, muscles, and gonads. Irreversible mass consists of all vital organs that are never subject to starvation such as bones, heart, and intestines. The ratio of reversible to irreversible mass is used as a measure of the condition of an individual. If the proportion of reversible mass becomes too low, individuals suffer increased mortality due to starvation. Maturation of individuals occurs at a fixed irreversible mass. In adult individuals, we assume that the standardized somatic mass is the irreversible mass plus a fixed fraction of irreversible mass.

TABLE 1. Variables and model parameters for Eurasian perch (*Perca fluviatilis*) feeding on a zooplankton resource (*Daphnia* sp., length 1 mm).

Variable and symbol	Value	Unit	Interpretation	Source†
Consumer variables				
N		no.	no. consumers in a school	
x		g	irreversible mass of a consumer	
y		g	reversible mass of a consumer	
Season				
Y	90	days (d)	length of year	
Ontogeny				
w_b	1.8×10^{-3}	g	egg mass	1, 2
x_f	4.6	g	maturation size	1, 2
q_J	0.74		maximum juvenile condition	3
q_A	1.37		maximum adult condition	15
k_r	0.5		gonad–egg conversion	
Planktivory				
α	0.62		allometric exponent	1, 2
$\hat{A}$	3.0×10^{-4}	L/d	maximum attack rate	4
w_{opt}	8.2	g	optimal forager size	5
Handling				
ξ_1	5.0	$d/g^{(1+\xi_2)}$	allometric scalar	2, 7
ξ_2	−0.8		allometric exponent	2, 7
Metabolism				
ρ_1	0.033	$g^{(1-\rho_2)}/d$	allometric scalar	8–11
ρ_2	0.77		allometric exponent	8–11
k_e	0.61		intake coefficient	8, 10–13
Mortality				
μ_0	0.01	d^{-1}	background rate of mortality	1, 2, 6
μ_J	varied	d^{-1}	additional juvenile background rate	
q_s	0.2		starvation condition	
s	1.0		starvation coefficient	
Resource				
r	0.1	d^{-1}	population growth rate	
K	100.0	L^{-1}	carrying capacity	14, 15
m	3.0×10^{-5}	g	wet mass, 1.0 mm *Daphnia*	1, 2

Notes: All parameters except Y, r, K, and m refer to individual-level processes.

† Sources: 1, Byström et al. (1998); 2, P. Byström (*unpublished data*); 3, Treasurer (1981); 4, Persson (1987); 5, Persson and Greenberg (1990); 6, B. Christensen (*unpublished data*); 7, Lessmark (1983); 8, Karås and Thoresson (1992); 9, Kitchell et al. (1977); 10, Elliott (1976); 11, Beamish (1974); 12, Solomon and Brafield (1972); 13, Rice et al. (1983); 14, E. Wahlström (*unpublished data*), 15, L. Persson (*unpublished data*).

Any reversible mass in excess of this fraction is considered gonad mass. We use this standardized somatic mass for size-dependent processes that are independent of the condition of individuals (de Roos et al. 2002). All individual level equations we use in our model are listed in Table 2.

For the resource consumption we use a Type II functional response, with a size-dependent attack rate and a size-dependent handling time. The attack rate is a hump-shaped function of consumer standardized mass, identical to the attack rate used in Persson et al. (1998), Claessen et al. (2000), and de Roos et al. (2002). Handling time of perch decreases with standardized somatic mass, due to gape and gut size increases. A discussion of the shape of the attack rate and handling time functions can be found in Persson et al. (1998) and de Roos et al. (2002). We assume that a school in compartment u spends 60% of its time foraging in that compartment, and 20% in each of the adjacent compartments. Biologically, this assumption reflects spatial wandering of schools on time scales smaller than we use for modeling consumer dispersal. Numerically, it avoids extreme differences between adjacent compartments, which are likely to introduce numerical artefacts. Including this assumption in the biomass zooplankton encounter rate leads to the function

$$\eta_u(w) = \sum_{\sigma=-1}^{1} A(w)P(\sigma)R_{u+\sigma}m \qquad (1)$$

which is the instantaneous biomass zooplankton encounter rate of a school j with standardized mass w, residing in compartment u. $P(\sigma)$ is the foraging distribution, with $\sigma = \{-1, 0, 1\}$ and $P(\sigma) = 0.6$ if $\sigma = 0$ and 0.2 otherwise, which is the fraction of foraging

TABLE 2. The *i*-state model equations.

Subject	Equation
Standardized mass	$w(x) = x(1 + q_J)$
Attack rate	$A(x) = \hat{A}\left\{\frac{w(x)}{w_{opt}} e^{[1-w(x)/w_{opt}]}\right\}^{\alpha}$
Food intake rate of a consumer in compartment *u*	$I_u(x) = \frac{\eta_u[w(x)]}{1 + H[w(x)]\eta_u[w(x)]}$
Handling time	$H(x) = \xi_1 w(x)^{\xi_2}$
Zooplankton encounter rate in compartment *u*	$\eta_u(x) = \sum_{\sigma=-1}^{1} A[w(x)]P(\sigma)R_{u+\sigma}m$
Energy balance	$E_g(x, y) = E_a(x) - E_m(x, y)$
Acquired energy	$E_a(x) = k_e I(x)$
Maintenance requirements	$E_m(x, y) = \rho_1(x + y)^{\rho_2}$
Fraction of energy used for growth in irreversible mass	$\kappa(x, y) = \begin{cases} \frac{1}{(1 + q_J)q_J}\frac{y}{x} & \text{if } x \leq x_f \text{ and } E_g > 0 \\ \frac{1}{(1 + q_A)q_A}\frac{y}{x} & \text{if } x > x_f \text{ and } E_g > 0 \\ 0 & \text{otherwise} \end{cases}$
Starvation mortality	$\mu_s(x, y) = \begin{cases} s(q_s x/y - 1) & \text{if } y < q_s x \\ 0 & \text{otherwise} \end{cases}$
Juvenile mortality	$\mu_J(x) = \text{varied}, \quad 0 \text{ if } x > x_f$
Total mortality	$\mu(x, y) = \mu_0 + \mu_s(x, y) + \mu_J(x)$
Fecundity	$F(x, y) = \begin{cases} k_r(y - q_J x)/w_b & \text{if } x > x_f \text{ and } y > q_J x \\ 0 & \text{otherwise} \end{cases}$

effort spent in compartment $u + \sigma$, which has resource density $R_{u+\sigma}$. We use the wet mass of a 1-mm *Daphnia* individual (m) to convert the zooplankton particle density to biomass density. Thus, total instantaneous biomass encounter rate is a weighted sum of biomass encounter rate in a school's present location and those adjacent to it. $A(w)$ is the hump-shaped size-dependent attack rate (Persson et al. 1998, and see Table 2 for equations). From the total energy intake, the basic metabolic costs are subtracted first. Any surplus energy intake that is left after individuals cover their basic metabolic costs goes into growth. A fraction of this energy is always converted into irreversible mass, independent of the condition of individuals. This fraction is larger for juvenile individuals than for adults, because adults allocate energy to gonads. A thorough discussion of this energy allocation rule can be found in Persson et al. (1998) and Claessen et al. (2000). All *i*-state functions described previously are listed in Table 2.

The attack rates, handling time, and energy allocation functions together define the size-based competitive relations in our model population. The parameter values in Table 1 imply that individuals with higher irreversible mass always have a higher minimum resource requirement (the resource level where total energy intake equals basic metabolic requirements) than smaller individuals. Thus, at the parameter settings we use, smaller individuals are competitively superior to larger individuals. Persson et al. (1998) show that this is a defining element of population dynamics of physiologically structured consumer–resource models.

Reproduction occurs once per year, at the start of the growing season. At these events, all gonad mass is removed from all adult consumers, and is converted to offspring.

We assume that all individuals suffer a constant background mortality. Juvenile individuals (individuals with standardized mass smaller than the maturation threshold) suffer an additional mortality rate. Any starvation mortality comes on top of this total background mortality.

We model dispersal of consumers as a random probabilistic process. Once per day all schools in the population move. The exact shape of the dispersal kernel is chosen for its computational convenience rather than its biological accuracy. The function describing this distribution is a piecewise quadratic polynomial (Eq. 3). For each school, we draw an uniformly distributed random number v between 0 and 3. We use the integral of the dispersal kernel and a rescaling procedure (Eq. 2) to calculate the new location L_{t+1} for each school:

$$L_{t+1} = L_t + \mathrm{int}\left[M_{\max}\frac{2}{3}\int_{n=0}^{v} M(n)\,dn - 1\right] \tag{2}$$

$$M(n) = \begin{cases} 0 & n < 0, n > 3 \\ \frac{1}{2}n^2 & 0 < n < 1 \\ -\frac{3}{2} + 3n - n^2 & 1 < n < 2 \\ \frac{9}{2} - 3n + \frac{1}{2}n^2 & 2 < n < 3. \end{cases} \tag{3}$$

This function is highly similar to the normal distribution, but has the advantage of having finite tails. The width of this dispersal kernel is controlled by a single parameter, $M_{\max}$. This is the maximum distance a school can move from one day to the next. Another advantage of using this particular shape is that the integral in Eq. 2 is generated by the sum of three uniformly distributed random variables (for a formal proof see Papoulis 1965). This obviously makes it very easy to simulate.

In this paper we study two values of the mobility of individuals, which we indicate as limited ($M_{\max} = 10$) and low ($M_{\max} = 1$) mobility. At limited mobility, individuals can move a maximum distance of one-fourth of the total size of the environment in one movement step. However, the chance of this occurring is ~0.001 per school per movement step. The average distance (independent of the direction) a school travels in one movement step is 2.7 compartments. At low mobility, each school has a two-thirds chance of staying where it is per movement event, and the average distance traveled is one-ninth of a compartment.

If we run the model with a large number of schools that all start in the same location, the spatial distribution at the end of the season gives us an intuitive notion of what these $M_{\max}$ values mean in terms of mixing. For limited mobility ($M_{\max} = 10$), the variance (mean squared displacement) of the spatial distribution after one season of movement is 120.56. In comparison, the variance for a uniformly distributed population is 126.79 (which is what we expect in the case of a well-mixed system). Hence, while on a daily scale movement is local, the limited mobility setting leads to an almost homogeneous system within one season. For low mobility ($M_{\max} = 1$), the variance is only 12.18, indicating that the distribution is far from uniform. The interaction between individuals and the environment at low mobility is local even on the timescale of seasons.

To confirm that our model is analogous to its nonspatial ancestors (such as Persson et al. 1998), we have constructed an approximation of such a well-mixed system, by setting the mobility parameter to a very high value ($M_{\max} = 100$). This leads to a completely random redistribution of schools over space at each movement occasion, a so-called mean-field approximation. While the effect of the consumer on the resource is local, the consumers spend so little time in one location that the local feedback of the resource on the consumer is lost. This parameter setting should result in dynamics that approach those of the nonspatial model, and thus allows us to link our model directly with existing theory for the dynamics of size-structured populations.

The environment

Each resource grows according to semi-chemostat dynamics, as described in Persson et al. (1998). Semi-chemostat dynamics is presumed to be an appropriate description for a resource population with small sizes that are invulnerable to predation. We further assume diffusive flow between resource compartments. Thus, resource dynamics for compartment u are given by

$$\frac{dR_u}{dt} = r(K - R_u) + D(R_{u+1} + R_{u-1} - 2R_u) - \sum_{\sigma=-1}^{1} P(\sigma)R_u \sum_{j\in\Lambda_{u-\sigma}} \frac{A(w_j)N_j}{1 + H(w_j)\eta_{u-\sigma}(w_j)} \tag{4}$$

where $\Lambda_{u-\sigma} = \{k \mid \text{school } k \text{ is in compartment } u - \sigma\}$.

The first term in Eq. 4 describes the dynamics of the edible fraction of a *Daphnia* population (semi-chemostat dynamics). This formulation of resource dynamics is identical to that used in Persson et al. (1998), Claessen et al. (2000), and de Roos et al. (2002). The second term is the discretized diffusion process of resources between adjacent compartments, which is controlled by the diffusion parameter D (we assume $D = 0.01d^{-1}$). The last term is the total consumption by the consumer population. $A(w)$, $H(w)$, and $\eta_i(w)$ are the size-dependent attack rate, handling time, and intake rate, respectively (equations are listed in Table 2). The set $\Lambda_{u-\sigma}$ gives the subset of all schools that forage in compartment u from compartment $u - \sigma$. Summing over all schools j in $\Lambda_{u-\sigma}$ for $\sigma = \{-1, 0, 1\}$ gives the total resource consumption in compartment u. Note that since we assume a circular space, u is only a relative index.

Population bookkeeping

Consumers are assumed to feed, grow (or shrink in case of starvation), and die continuously, but reproduce only at the start of a growth season in a sharply pulsed event. Furthermore, movement of schools through the environment is a discrete probabilistic process. The model is thus a combination of a continuous dynamical system, describing growth and survival of the consumers and production and consumption of the resource during the growth season, and a discrete map describing the movement and reproduction of consumers. Numerically, the model can be studied using the EBT (Escalator Boxcar Train) framework (de Roos et al. 1992, Persson et al. 1998). The EBT method is specifically designed to handle the numerical integration of the equations that occur in physiologically structured models. Next follows a description of how the EBT method is applied to keep track of the consumer population in our model.

The pulsed reproduction process ensures that there exists a natural subdivision of the population into cohorts of individuals. At the beginning of each growth season, all gonad mass is removed from all adults, and converted to a number of offspring, which make up a cohort or year class. These newborn individuals are allocated to a fixed number of newly formed schools, which are added to the population. In the current study, we added 100 newborn schools per reproduction event, irrespective of the number of offspring involved. Tests where we varied this number have shown that 100 is large enough to allow for variation between schools, but still computationally feasible. All newborn individuals are identical in all respects except their location in space. Each new school is assigned a random initial location. In the similar models studied previously (Persson et al. 1998, Claessen et al. 2000, de Roos and Persson 2001, de Roos et al. 2002), all newborn individuals are pooled into one large cohort of individuals, which are identical throughout their life history. The introduction of schools is a modification of the EBT algorithm. By breaking each reproductive pulse into independent schools, we allow life-history variation between individuals of the same age to develop. While variation between schools may develop, *within* schools all individuals are identical, and remain so for the duration of their life.

The discrete nature of the population distribution in the *i*-state space allows us to describe each school with a set of differential equations. For each school in the population, we need one differential equation to describe the change of each *i*-state variable, and an additional one that describes the number of individuals in the school. The dynamics of the entire consumer population, both in terms of its abundance and its composition, can be followed throughout the growth season by numerically integrating this system of ordinary differential equations for each cohort separately. Changes in the resource population are calculated by simultaneously integrating Eq. 4. At the end of each day, the integration is interrupted, and the movement of schools of consumers is processed.

Overall, the simulation of physiologically structured populations thus involves the numerical integration of a (large) system of ordinary differential equations, which is extended in dimension at the beginning of each season with a concurrent reset of some of the variables. The dimension of the system is reduced whenever the number of individuals in a given cohort has become negligible, at which time the differential equations for such a cohort are removed.

RESULTS

The population dynamics of the mean-field model (as approximated by $M_{\max} = 100$, Fig. 1) show the typical single cohort cycles, which are discussed in detail by Persson et al. (1998). Reproduction occurs in large bursts, once every seven years for the parameters used in Fig. 1. The newborn cohorts reduce the resource to such low levels that they themselves barely survive, and all larger individuals in the population starve and die. Scramble competition for food leads to a very slow increase in size of individuals in these year classes. Death in these large year classes occurs due to background mortality. This leads to a gradual release of scramble competition, since there are less and less individuals to share the available food with. Body growth speeds up as the number of individuals decreases. During their sixth year, the individuals reach maturation size, and start allocating mass to gonads. At the first possible occasion, their seventh birthday, reproduction takes place, a new dominant cohort monopolizes the resource, and the cycle starts again. When juvenile background mortality (μ_J) increases, the decrease in numbers speeds up, which causes a quicker release of competition. Eventually, the timing of maturation shifts over a year boundary. When this happens, individuals can reproduce one year earlier, and the length of the cycle shortens by one year. Hence, we expect a pattern of stepwise decrease in the period of the cycle, until at a certain juvenile background mortality, individuals mature within one growth season, and reproduce when they are one year old. When mortality increases even more, the population eventually goes extinct.

The above shows the pivotal role of the juvenile mortality parameter μ_J in shaping the dynamics of size-structured consumers. Juvenile mortality is also a parameter for which we have no empirically determined value. Such a value is hard to obtain, since it represents all mechanisms (predation, disease, and other factors) that make juvenile individuals more likely to die than adults. In this paper we focus on the relation of decreasing single cohort cycle length with increased juvenile mortality. This relation is well documented for similar systems (Persson et al. 1998, de Roos and Persson 2001, de Roos et al. 2002) and is clearly present in our mean-field approximation. Based on this similarity we conclude that our model results at lower mobility can be attributed to the consequences of space-induced individual variation.

Limited mobility

The bifurcation diagram at limited mobility ($M_{\max} = 10$, Fig. 2A) is highly similar to both that of a nonspatial variant of the model and our well-mixed version. Fig. 2A is constructed by calculating time series for a large number of values of juvenile additional mortality (μ_J). After removal of transient dynamics, the population is sampled at the beginning of each season, and the number of non-newborn individuals is plotted. Thus, the one-year cycle at high juvenile mortality shows as a single dot in the graph (the population state is the same each year), the two-year cycle shows up as two points (one for the high and one for the low year) and so on. The period of the cycles varies from one year at high juvenile mortality to a seven-year cycle, identical to

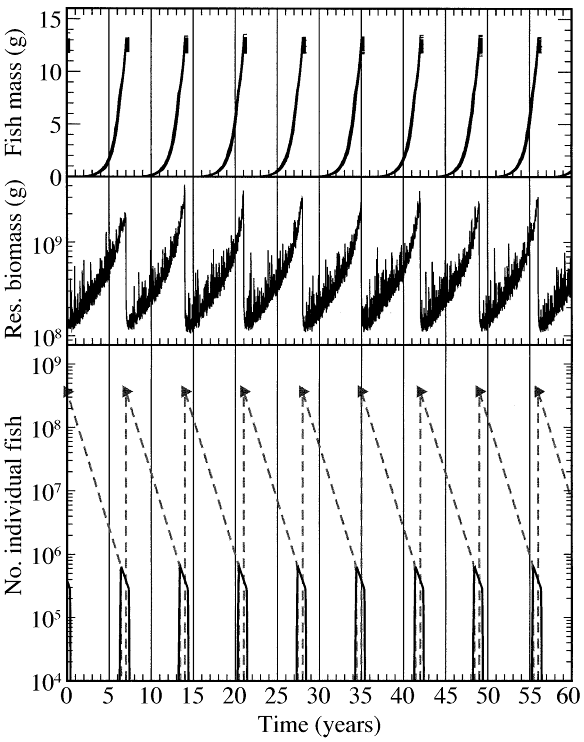

FIG. 1. Single cohort cycles generated by the model with high mobility. The upper panel shows the growth curves of schools (standardized mass), the middle panel shows the resource (res.) biomass dynamics, and the lower panel shows the numbers of individuals in the population. In the lower panel, triangles represent newborn individuals, dashed lines are juveniles, and solid lines indicate the number of adults in the population. Parameter settings for this realization are $\mu_J = 0.001$ and $M_{max} = 100$; all other parameters are as in Table 1.

that in Fig. 1. Small regions of noisy and irregular dynamics are located at the boundaries where the period of the single cohort cycles shifts. These ''interperiodic'' areas are also found by Persson et al. (1998) and de Roos et al. (2002), even though they use a fully deterministic model. They are due to the fact that at parameter values close to the period transition, the maturation age alternates between two consecutive values. The only alternative attractor that coexists with the single-cohort cycles for a significant parameter range is the one-year cycle present at $0.044 \leq \mu_J \leq 0.073$. Extensive examination of model dynamics for the limited mobility model have revealed that there is no divergence in the life history of individuals. Apparently, limited mobility creates enough randomization for all individuals to experience approximately the same environment and thus all individuals have approximately equal life histories.

Low mobility

Decreasing mobility to $M_{max} = 1$ significantly changes the dynamics of the population (Fig. 2B). At low mobility the clear relation between juvenile mortality and cycle length disappears. The bifurcation shows two qualitatively different regions. At low juvenile mortality ($\mu_J < 0.015$), the dynamics appear noisy and aperiodic. At higher μ_J, it is more regular, and corresponds more clearly to dynamics at higher mobility. The cycles with a three-, two-, and one-year period can be clearly distinguished. The maximum value of μ_J is also unchanged at low mobility. Below we examine in more detail the periodic dynamics at high juvenile mortality, and the seemingly aperiodic dynamics at low juvenile mortality.

Periodic dynamics.—The cyclic dynamics at $\mu_J = 0.03$ is very similar to the dynamics expected from the mean field approximation and its nonspatial archetype (Fig. 3 and Persson et al. 1998). There is a dominant pulse of newborns that is generated every second year ($t = 1, 3, 5, \ldots$). At lower juvenile mortality, the cycle length changes to three years, and the dynamics bear the same resemblance to the mean field dynamics. Even when mobility is greatly reduced, the population dynamics exhibited by the model is roughly identical to

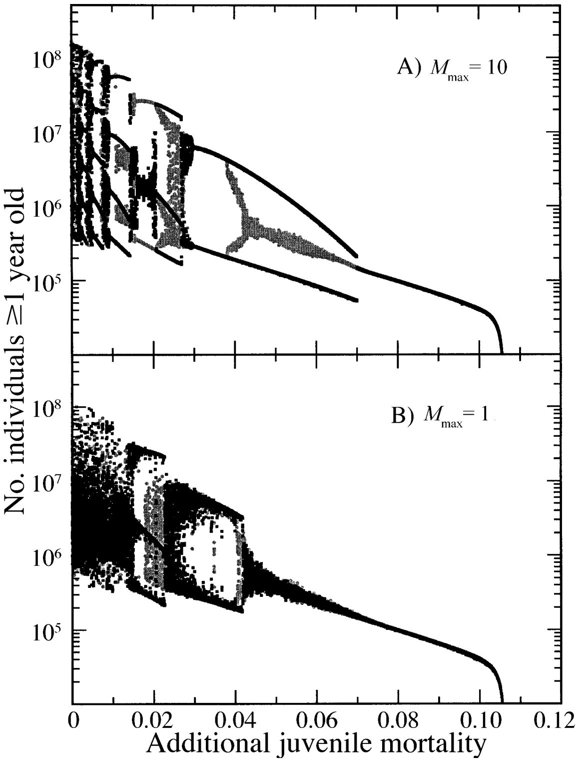

FIG. 2. Numerical bifurcation diagram of the one-year and older consumer population, varying additional juvenile mortality for (A) limited mobility ($M_{max} = 10$) and (B) low mobility ($M_{max} = 1$). The population is sampled once per year, at the beginning of the season. Each dot in the graph represents a sampling occasion. The black symbols indicate the state of the system when the bifurcation is started at zero additional juvenile mortality and then increased; the gray symbols show the same plot when mortality is reduced, starting at 0.1. For clarity, newborn individuals are omitted.

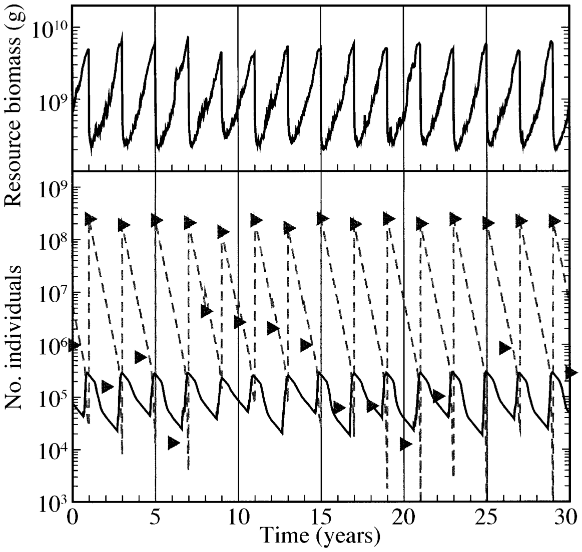

FIG. 3. Single cohort cycles generated by the low-mobility model. Parameter settings for this realization are μ_J = 0.03 and M_{max} = 1; all other parameters are as in Table 1. The upper panel shows the dynamics of the resource, the lower panel that of the consumer. Triangles represent the newborn individuals, dashed lines are juveniles, and solid lines represent the number of adults in the consumer population.

that of the well-mixed model, indicating strong robustness of the mechanism that causes the single cohort cycles to the stochasticity induced by low mobility. On the individual level however, considerable variation is present (Fig. 4). At t = 9, a large year class is born (marked in black in Fig. 4). Initially, this year class shows the life history corresponding to cohort cycles, with very slow growth due to low resource levels. Over time, the number of individuals drops and the resource recovers, speeding up individual growth. This leads to a roughly exponentially shaped initial growth trajectory. Over time, variation between schools increases. At the age of two years (t = 11) the cohort is mature, and produces a new large recruitment pulse (again marked in black in Fig. 4). This new year class again depresses the resource to a low level. The high juvenile mortality and high local variation in resource density ensure that not all the adult schools are outcompeted (Fig. 3). Instead, the growth of these adults is effectively stopped. Some of the adults can reproduce once more in later years, but their contribution to the total reproduction is marginal. Fig. 4 shows that although the cyclicity apparent from the population dynamics (Fig. 3) is clearly reflected in the individual life histories, the high level of stochasticity induced by the low mobility facilitates extensive variation in life history between individual schools within year classes, which leads to frequent coexistence of adults from several different year classes.

Aperiodic dynamics.—At low juvenile mortality, there is no clear fixed-length cycle that dominates the dynamics (Fig. 5). On a longer time scale, an alternation between two dynamical modes develops: irregular dynamics (t = 7–17 and t = 32–26) alternate with cohort cycle-like dynamics. In the intervals of irregularity, the population exhibits dynamics that appear

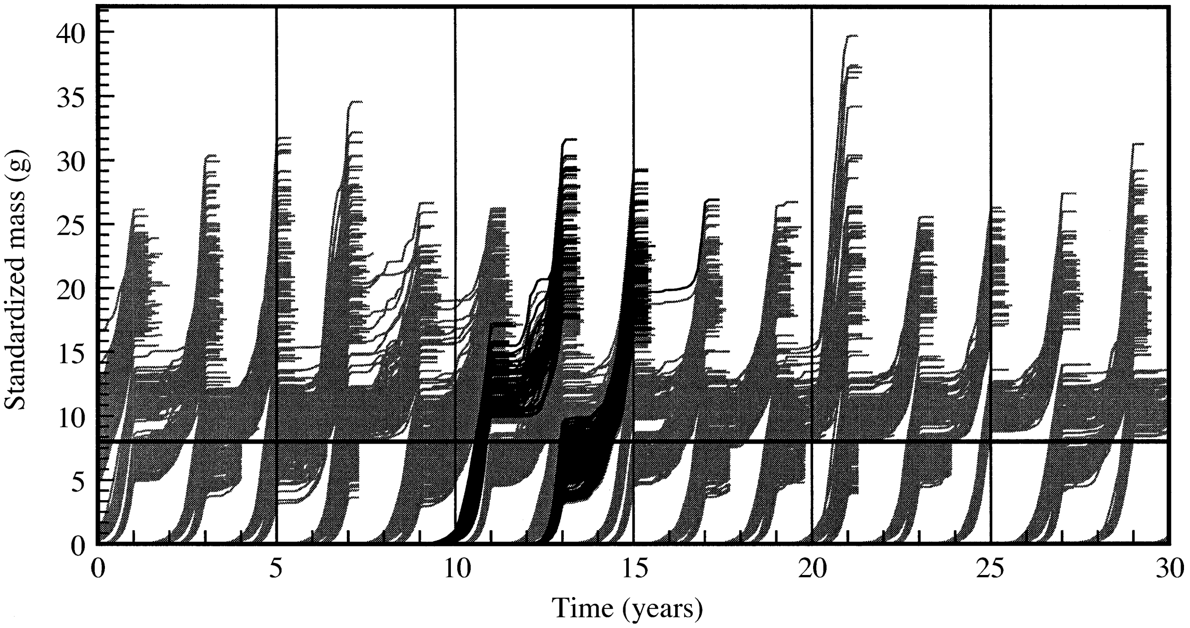

FIG. 4. Growth curves of individuals in the two-year cycles corresponding to the realization in Fig. 3. Each line depicts the growth trajectory of one school of individuals. Lines end when the number of individuals in the school falls below 1. Parameter settings for this realization are μ_J = 0.03 and M_{max} = 1, all other parameters as in Table 1. The year classes shown in black are representative of the different life histories experienced by individuals in the population.

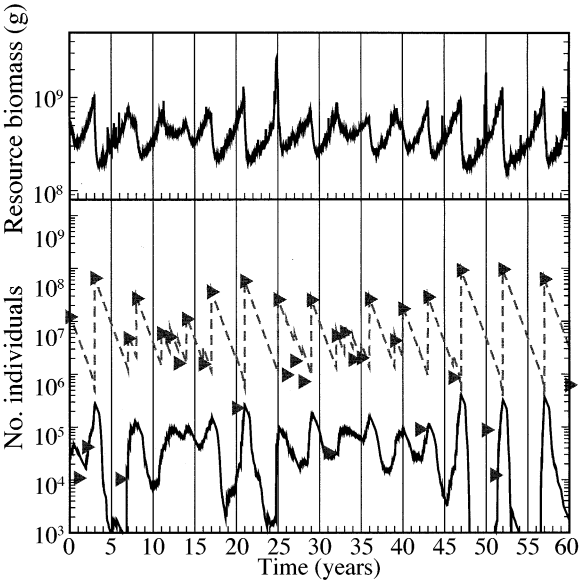

FIG. 5. Dynamics of the model population at low mobility and low juvenile mortality ($\mu_J = 0.001$ and $M_{max} = 1$). All other parameters are as in Table 1. The upper panel shows the dynamics of the resource, the lower panel that of the consumer. The triangles represent the newborn individuals, dashed lines are juveniles, and solid lines represent the number of adults in the population.

highly stochastic. Reproduction occurs practically every year in this time span, and fluctuations in the resource are small, indicating that there is no single dominating year class. Eventually, a very large pulse of recruits is born, which strongly decreases the resource. Such a mass-reproduction event marks the beginning of a time interval of highly cyclic dynamics. The cyclicity eventually breaks down again due to stochasticity, until the next mass reproduction. In Fig. 5, several dynamical mode switches are present. At $t = 17$, mass reproduction occurs. Until $t = 32$, a large year class arises every fourth year, which is clearly reflected by the strong periodicity in the resource dynamics. Around year 32 the cyclicity breaks down, until at $t = 36$ there is again a strong pulse of offspring, which outcompetes most other individuals. The dynamics become more regular again, eventually leading to a type of dynamics very similar to single cohort cycles with a period of five years (from $t = 47$ onward). Some adults survive from one period to the next, but only in small numbers. Clearly, the competitive relations that lead to single cohort cycles in better mixed models have a strong influence on the dynamics, even at low mobility.

In addition to the population effects, the individual level dynamics is significantly affected by the induced stochasticity (Fig. 6). In general, a large range of sizes is present in the population. The size-based difference in competitive ability is visible. Each newborn year class grows to "catch up" with the broad band of sizes

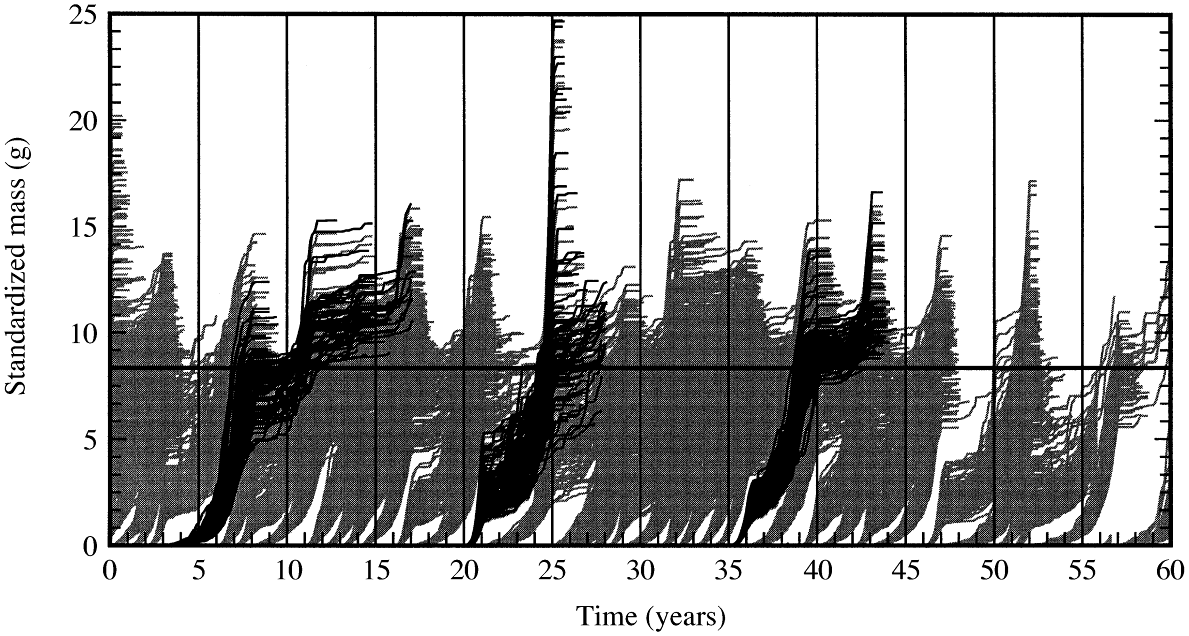

FIG. 6. Growth curves of individuals at low additional juvenile mortality ($\mu_J = 0.001$) and low mobility ($M_{max} = 1$), corresponding to the dynamics shown in Fig. 5. Each line depicts the growth trajectory of one school of individuals. Lines end when the number of individuals in the school falls below 1. All other parameters are as in Table 1. The schools from three year classes with distinctly different life-history trajectories are marked black.

formed by the rest of the population. The three year classes (born at $t = 3$, $t = 20$, and $t = 35$) marked in black in Fig. 6 are illustrations of the large variation that exists both within and between year classes. The large offspring cohort born at $t = 3$ initially grows slowly. Eventually, growth speeds up as the number of individuals decreases. This pattern of increasing growth rate is reminiscent of the growth patterns observed in the single cohort cycles. The variation between individuals from this year class is small initially, but increases as growth speeds up. At age 5 ($t = 8$), individuals from this year class range from 4-g juveniles to 12-g adults. Eventually the individuals born at $t = 3$ reach a mass of up to 16 g, and live for up to 14 years. In contrast, individuals born in the small year class born at $t = 20$ may reach up to 25 g, and do so in a much shorter time (they reach their maximum size in six years, as opposed to 10 years for their $t = 3$ ancestors). Shortly after birth, large variation in mass develops between schools born at $t = 20$. However, before maturation this initial variation decreases again. The year class produced at $t = 35$ exhibits a rather different life-history trajectory. After a very short interval of slow growth, these individuals grow quickly until reaching maturity. After maturation, some divergence in size occurs. Eventually, these individuals reach a maximum size of ∼17 g, at an age of 10 years. This high variation over time illustrates the whimsical environment that individuals experience.

DISCUSSION

This paper deals with the interaction between overall population dynamics and life history of individuals, in particular the variation between individuals that are born at the same time. Such individuals have experienced the same global, but not necessarily local environment. In the absence of divergence between individuals born at the same time, the model predicts single cohort or generation cycles, which are the most predominant type of cyclic population dynamics, according to a recent analysis in Murdoch et al. (2002). This goes to show that although we use perch as a model organism, our results are applicable beyond the specific field of perch population dynamics. In these generation cycles, individual life histories become highly synchronized. The generality of our work comes from the fact that we address the question of how robust these cycles are against the buildup of variability and the consequent breakdown of the life-history synchrony. We use the spatial component merely as a way to facilitate the stochasticity that leads to life-history divergence among individuals of the same age.

The global reproduction process that we use can arguably be viewed as a reasonable approximation of the reproductive process of egg-laying species without extensive parental care, where the location of a parent is not tightly coupled to the place of birth of its young. More important, treating reproduction as a global process prevents the formation of spatial patterns. We study the occurrence and effects of divergence of initially similar individuals resulting from stochasticity. The possible spatial pattern formation associated with local reproduction would greatly complicate the mechanisms leading to the model dynamics, clouding the interplay between the stochasticity-induced individual variability and the single cohort cycle dynamics, which is the focus of this study.

Both the dynamics and the bifurcation pattern of our model correspond well to earlier deterministic models of size-structured populations (Persson et al. 1998, Claessen et al. 2000, de Roos and Persson 2001, de Roos et al. 2002) when we use parameter settings that approximate a well-mixed system. By reducing mobility of individuals we allow stochastic variation to develop. In our limited mobility scenario ($M_{\max} = 10$, Fig. 2A), we find no effect on either population dynamics or the individual level. This is surprising considering the mechanism that drives the cycles. For single cohort cycles to occur, newborn year classes must depress the resource to such low levels that the ‘‘parent’’ year classes starve, or at least remain in a bad condition, unable to reproduce. Intuitively, this condition could be sensitive to limited mixing. When the schools that make up a year class of newborns are not homogeneously distributed in space, some more fortunate schools of adults may survive the period of low resource availability following the birth of a large offspring cohort. These surviving adults could then reproduce in ‘‘off-beat’’ years, and in principle cause the collapse of the recruit-driven cycles. However, the only effect we find on the population dynamics when mobility is limited, is an increase in the duration of transient dynamics (not shown), and a widening of the interperiodic attractors at period shifts of the cycles.

When mobility of individuals is low ($M_{\max} = 1$), the bifurcation structure of the model changes considerably. It can roughly be divided into two areas. One characterized by noisy, irregular dynamics at low juvenile mortality, the other at high juvenile mortality where the cyclic dynamics is still apparent. The border between these regions falls at the transition from three- to four-year cycles. All recruit-driven cycles with a period larger than three years seemingly disappear, and cycles with period two and three years persist. While on a population level these cycles are similar to recruit-driven cycles, they exist despite considerable variation in the life history of individuals, and a population that consists of several year classes simultaneously, spanning a wide range of sizes. This discrepancy between the orderly dynamics at the population level and the large variation between individuals within year classes shows that differences between individuals are not always important factors in determining population dynamics, a view which is strongly advocated in several influential papers (Huston et al. 1988, DeAngelis et al. 1993, Rice et al. 1993).

At lower juvenile mortality, the periodicity in the model dynamics apparently disappears. However, closer analysis shows that the mechanisms that drive the population dynamics are the same as those found at high or intermediate mobility. Large newborn cohorts have a strong effect on the resource, preventing or strongly hampering the reproduction in the years following their birth. They also cause large scale starvation among larger individuals. At low mobility, cycles tend to break down due to high stochasticity. Consecutively, the competitive advantage of small individuals leads to convergence in size of individuals of (weak) offspring cohorts. Eventually this culminates in a high number of adults in the population, which produce a large pulse of offspring that temporarily dominates the resource and thus population dynamics.

DeAngelis et al. (1993) study the influence of stochasticity in growth rates of individuals on the dynamics of a fish cohort. They show that stochastic perturbation of these rates over time per se has no significant effect on the developing size distribution of the cohort. However, if the stochastic variation is correlated positively with size (i.e., larger individuals on average have a larger growth rate), then the cohort size distribution significantly widens. In our current work, we assume a positive relation between attack rate and size for the entire juvenile size range. Hence, in this respect, our model corresponds to that of DeAngelis et al. (1993); when food is not limiting, larger individuals grow faster than smaller individuals. However, we consider the complete population dynamical feedback loop, including the resource dynamics. In our model, while a larger size is generally associated with a larger attack rate, it is by no means a guarantee for faster growth. Realized growth rates of individuals depend crucially on the resource density that individuals encounter. In previous work (Persson et al. 1998, de Roos and Persson 2003) it has been demonstrated that this population dynamical feedback loop plays a defining role in shaping multigenerational population dynamics, and in this study we show that the same feedback is a strong regulatory force in intra-cohort dynamics and variation as well, even when mobility of individuals is strongly limited.

De Roos et al. (2002) and Rice et al. (1993) study the effects of flexible habitat choice of a size-structured consumer population. In addition to a large, profitable habitat with high juvenile mortality, their model incorporates a small, less profitable habitat, which is also less dangerous to juveniles that continuously choose their habitat based on a profitability vs. mortality risk criterion. In this system, individual variability could in principle develop when different juveniles grow up in habitats of different profitability. De Roos et al. (2002) show that juveniles distribute themselves such that each habitat has approximately equal profitability. This equal profitability is attained through the effect of these juveniles on the resource density. Hence, in their model, the occurrence of individual variability is constrained by the population dynamical feedback.

Our results show a similar effect, in that at low mobility and mortality, it is the accumulation of variation between individuals that eventually leads to a large pulse of offspring, which synchronizes population dynamics and reduces variability. In other words, the individual variability not only affects the population dynamics, it can actually be considered to amplify the effect of the population dynamical feedback loop to such an extent that it eventually resets the variability in the consumer population. Our intuitive expectation that individual variability would weaken the effects of size-based competition and hence would lead to the disappearance of single cohort cycles is contradicted by our results. While the single cohort cycles do break down, the size-based mechanisms that shape the dynamics of the population are to a large extent the same mechanisms that are important in nonspatial versions of the model. The apparent change in the bifurcation structure of the model at low mobility can on a short time scale be fully explained in terms of the mechanisms that Persson et al. (1998) identify as building blocks of the single cohort cycles. On a longer time scale a new phenomenon appears in the dynamics. A dynamical pattern similar to single cohort cycles gradually becomes less regular, accompanied by an upward trend in the number of adults in the population. This eventually leads to strong recruitment and a temporary reinstatement of the single cohort cycle regime. The phenomenon can be explained by a superposition of two main components of the model, the original deterministic model and the stochasticity induced by local interactions. While the complexity of the model dynamics may seem intimidating, it can be fully understood by a combination of the model components. At the parameter values we have studied, there are no new emergent properties in the dynamics of the model population. This result illustrates the importance of the type of understanding that is gained by studying deterministic simplifications of natural systems, as the knowledge of the mechanisms that shape population dynamics of the deterministic analogue of our model (Persson et al. 1998), allows us to understand the apparent complexity of the dynamics discussed here.

One of the features of individual based simulation models (IBSMs) that we have not addressed is the fact that they often deal with small population sizes. Our analysis does not cover such situations, and hence our conclusions can not be applied. In such cases, stochasticity may play a more important role than for the population studied here. Another argument that is often considered a boon of the IBSM approach and that is often used to advocate it, is the interaction between individuals and the environment, which is considered on a local scale (for references see the review by Grimm 1999). Here, we have extensively studied the effects of the stochasticity induced by such local interactions in the context of single cohort cycles, and we find little influence on the mechanisms that shape population dynamics. Although we have studied the effects of only one kind of stochasticity, our results indicate that it should not be taken as self-evident that individual variability has a major impact on population dynamics and persistence in all contexts.

ACKNOWLEDGMENTS

We thank Bill Gurney and two anonymous reviewers for helpful comments on earlier versions of the manuscript. A.M. de Roos is supported by a grant from the Netherlands Organization for Scientific Research (NWO). L. Persson is financially supported by grants from the Swedish Research Council and the Swedish Research Council for Environment, Agricultural Sciences, and Spatial Planning.

LITERATURE CITED

Beamish, F. W. H. 1974. Apparent specific dynamic action of largemouth bass, *Micropterus salmonides*. Journal of the Fisheries Research Board of Canada **31**:75–87.

Byström, P., L. Persson, and E. Wahlström. 1998. Competing predators and prey: juvenile bottlenecks in whole-lake experiments. Ecology **79**:2153–2167.

Claessen, D., A. M. de Roos, and L. Persson. 2000. Dwarfs and giants: cannibalism and competition in size-structured populations. American Naturalist **155**:219–237.

DeAngelis, D. L., D. C. Cox, and C. C. Coutant. 1979. Cannibalism and size dispersal in young-of-the-year largemouth bass: experiments and model. Ecological Modelling **8**:133–148.

DeAngelis, D. L., K. A. Rose, L. B. Crowder, E. A. Marschall, and D. Lika. 1993. Fish cohort dynamics—application of complementary modeling approaches. American Naturalist **142**:604–622.

de Roos, A. M. 1989. Daphnids on a train: development and application of a new numerical method for physiologically structured population models. Ph.D. thesis. Leiden University, Leiden, The Netherlands.

de Roos, A. M., O. Diekmann, and J. Metz. 1992. Studying the dynamics of structured population models: a versatile technique and its application to *Daphnia*. American Naturalist **139**:123–147.

de Roos, A. M., K. Leonardsson, L. Persson, and G. G. Mittelbach. 2002. Ontogenetic niche shifts and flexible behaviour in size-structured populations. Ecological Monographs **72**:271–292.

de Roos, A. M., and L. Persson. 2001. Physiologically structured models—from versatile technique to ecological theory. Oikos **94**:51–71.

de Roos, A. M., and L. Persson. 2003. Competition in size-structured populations: mechanisms inducing cohort formation and population cycles. Theoretical Population Biology **63**:1–16.

Dong, Q., and D. L. DeAngelis. 1998. Consequences of cannibalism and competition for food in a smallmouth bass population: an individual-based modeling study. Transactions of the American Fisheries Society **127**:174–191.

Ebenman, B., and L. Persson, editors. 1988. Size-structured populations: ecology and evolution. Springer-Verlag, Berlin, Germany.

Elliott, E. M. 1976. The energetics of feeding, metabolism and growth of brown trout (*Salmo trutta* L.) in relation to body weight, water temperature and ration size. Journal of Animal Ecology **45**:923–948.

Grimm, V. 1999. Ten years of individual-based modelling in ecology: what have we learned and what could we learn in the future? Ecological Modelling **115**:129–148.

Gurney, W. S. C., D. A. J. Middleton, R. M. Nisbet, E. McCauley, W. W. Murdoch, and A. de Roos. 1996. Individual energetics and the equilibrium demography of structured populations. Theoretical Population Biology **49**:344–368.

Huston, M., D. DeAngelis, and W. Post. 1988. New computer-models unify ecological theory. BioScience **38**:682–691.

Karås, P., and G. Thoresson. 1992. An application of a bioenergetics model to eurasian perch (*Perca fluviatilis* L.). Journal of Fish Biology **41**:217–230.

Kitchell, J. F., D. J. Stewart, and D. Weininger. 1977. Applications of a bioenergetics model to yellow perch (*Perca flavescens*) and walleye (*Stizostedion vitreum vitreum*). Journal of the Fisheries Research Board of Canada **34**: 1922–1935.

Lessmark, O. 1983. Competition between perch (*Perca fluviatilis*) and roach (*Rutilus rutilus*) in South Swedish lakes. Ph.D. thesis. University of Lund, Lund, Sweden.

Lindström, T. 1955. On the relation fish size–food size. Reports from the Institute for Freshwater Research Drottningholm **36**:133–147.

McCauley, E., R. M. Nisbet, A. M. de Roos, W. W. Murdoch, and W. S. C. Gurney. 1996. Structured population models of herbivorous zooplankton. Ecological Monographs **66**: 479–501.

Metz, J., and A. M. de Roos. 1992. The role of physiologically structured population models within a general individual-based modelling perspective. Pages 88–111 *in* D. DeAngelis and L. Gross, editors. Individual-based models and approaches in ecology. Chapman and Hall, New York, New York, USA.

Metz, J., A. M. de Roos, and F. van den Bosch. 1988. Population models incorporating physiological structure: a quick survey of the basic concepts and an application to size-structured population dynamics in waterfleas. Pages 106–126 *in* B. Ebenman and L. Persson, editors. Size-structured populations: ecology and evolution. Springer-Verlag, Berlin, Germany.

Metz, J., and O. Diekmann, editors. 1986. The dynamics of physiologically structured populations. Springer-Verlag, Berlin, Germany.

Murdoch, W. W., B. E. Kendall, R. M. Nisbet, C. J. Briggs, E. McCauley, and R. Bolser. 2002. Single-species models for many-species food webs. Nature **417**:541–543.

Murdoch, W. W., R. M. Nisbet, E. McCauley, A. M. de Roos, and W. S. C. Gurney. 1998. Plankton abundance and dynamics across nutrient levels: tests of hypotheses. Ecology **79**:1339–1356.

Pacala, S. W., and J. A. Silander. 1985. Neighborhood models of plant population dynamics. I. Single species models of annuals. American Naturalist **125**:385–411.

Papoulis, A. 1965. Probability, random variables and stochastic processes. McGraw-Hill, New York, New York, USA.

Persson, L. 1987. The effects of resource availability and distribution on size class interactions in perch, *Perca fluviatilis*. Oikos **48**:148–160.

Persson, L., and L. A. Greenberg. 1990. Optimal foraging and habitat shift in perch, *Perca fluviatilis* in a resource gradient. Ecology **71**:1699–1713.

Persson, L., K. Leonardsson, A. M. de Roos, M. Gyllenberg, and B. Christensen. 1998. Ontogenetic scaling of foraging rates and the dynamics of a size-structured consumer-resource model. Theoretical Population Biology **54**:270–293.

Rice, J. A., J. E. Breck, S. M. Bartell, and J. F. Kitchell. 1983. Evaluating the constraints of temperature, activity and consumption on growth of largemouth bass (*Micropterus salmoides*). Environmental Biology of Fishes **9**:263–276.

Rice, J. A., T. J. Miller, K. A. Rose, L. B. Crowder, E. A. Marschall, A. S. Trebitz, and D. L. DeAngelis. 1993. Growth-rate variation and larval survival—inferences from an individual-based size-dependent predation model. Canadian Journal of Fisheries and Aquatic Sciences **50**:133–142.

Schmitz, O. J. 2000. Combining field experiments and individual-based modeling to identify the dynamically relevant organizational scale in a field system. Oikos **89**:471–484.

Schmitz, O. J., and G. Booth. 1997. Modelling food web complexity: the consequences of individual-based, spatially explicit behavioural ecology on trophic interactions. Evolutionary Ecology **11**:379–398.

Solomon, D. J., and A. E. Brafield. 1972. The energetics of feeding, metabolism and growth of perch (*Perca fluviatilis* L.). Journal of Animal Ecology **31**:699–718.

Thompson, W. A., I. Vertinsky, and J. R. Krebs. 1974. The survival value of flocking in birds: a simulation model. Journal of Animal Ecology **43**:785–820.

Treasurer, J. W. 1981. Some aspects of the reproductive biology of perch Perca fluviatilis: fecundity, maturation and spawning behavior. Journal of Fish Biology **18**:729–740.

Tyler, J. A., and K. A. Rose. 1994. Individual variability and spatial heterogeneity in fish population-models. Reviews in Fish Biology and Fisheries **4**:91–123.